DINAME 2017 - Proceedings of the XVII International Symposium on Dynamic Problems of Mechanics
A. T. Fleury, D. A. Rade, P. R. G. Kurka (Editors), ABCM, São Sebastião, SP, Brazil, March 5-10, 2017

Dynamics of Embarked Vibrating Systems

Luiz Fabiano Damy[1], **Everton Spuldaro**[1], **Domingos Alves Rade**[1]

[1] Technological Institute of Aeronautics (ITA), Division of Mechanical Engineering, São José dos Campos, SP, Brazil
lfdamy@gmail.com, evertonspuldaro@gmail.com, rade@ita.br.

Abstract: In many practical situations, especially those in the field of aeronautical and aerospace engineering, vibrating systems are very often embarked in vehicles (fixed-wing airplanes, helicopters, satellites, space launchers, etc.), which can perform manoeuvers comprising general translations and rotations. In such cases, it is of primary interest to characterize the motion of the embarked vibrating systems with respect to reference systems fixed to the vehicles, which are thus characterized as non-inertial reference frames. Under this motivation, this paper brings a fundamental study on this problem, by addressing a methodology for the modelling of vibration motion of linear systems with respect to non-inertial reference frames, based on the concept of inertia force. First, the expressions of the four components of inertia forces are obtained for a particle in motion with respect to non-inertial reference frame undergoing general three-dimensional motion. Those equations are then particularized for a single-mass, three degree of freedom oscillator embarked in a vehicle undergoing general motion in space and simplified further for the case of a single-mass, two degree-of-freedom oscillator embarked in a vehicle performing rotation about a fixed axis. For this later case, the free and forced vibration motions are considered. Numerical simulations are performed to demonstrate the influence of the vehicle motion on the dynamic behavior of the vibrating systems, in terms of vibration response and stability.

Keywords: non-inertial reference frames, embarked systems, inertia forces

INTRODUCTION

In many situations of practical interest, vibrating systems can be found embarked in other bodies, named herein *vehicles*, which can undergo arbitrary motion in space. In such cases, one possibility is to model the dynamic behavior of the vibrating system with respect a fixed reference frame (or, more generally, an *inertial reference frame*) by using the fundamental principles of Newtonian Mechanics or Analytical Mechanics. However, very often (possibly mostly often), the interest resides in the characterization of the dynamics of the vibrating systems with respect to the vehicles or, equivalently, with respect to a *non-inertial reference frames* attached to these latter. Since the dynamic behavior can be significantly different in either case, it is of utmost importance to model the behavior of vibrating systems with respect to the vehicle-based reference frames, accounting for the most general form of motion that the vehicle can perform.

In engineering practice, discrete and continuous vibrating systems can be found embarked in a variety of vehicles, such as aircraft and spacecraft. Some of them are integral parts of the vehicle, such as structural components or appendages (flexible solar panels or antennas, for example) or parts of propulsion systems (fan blades, helicopter rotor blades, propeller blades, for example); alternatively, they can be devices voluntarily attached to the vehicle in order to perform specific functions related to their dynamic responses. For this latter case, dynamic vibration absorbers (DVAs) and inertial sensors are remarkable examples.

For illustration, Fig. 1 depicts two types of DVAs frequently found in helicopters; the first (Fig.1(a)) is intended to attenuate vibrations of a three-blade helicopter main rotor, while the second (Fig. 1(b)) is used to attenuate vibrations of the helicopter fuselage, being frequently positioned below the pilot seat (Krysinksi and Malburet, 2007).

In the examples discussed above, the vibrating systems are essentially of discrete nature (in the example considered in Fig. 1(b) the inertia of the beam is small w.r.t. the tip mass, so that the system behaves as an equivalent single-degree-of-freedom in the frequency band of interest). However, a variety of problems involve vibrations of continuous systems embarked in vehicles, of which two examples are shown in Fig. 2. Figure 2(a), illustrates a *tuning fork gyroscope*, which belongs to the broader category of inertial sensors known as *Coriolis gyroscopes*, which are intended to provide measurements of the rotation speed of the vehicles to which they are attached (Apostolyuk, 2016). They underlying principle is the coupling between the dynamic response of the vibrating element and the rotation speed of the vehicle, indicated by Ω. Another example is shown in Fig. 2(b), consisting of an artificial satellite containing flexible solar panels, which vibrate which respect to the satellite body when attitude maneuvering is performed. As those elastic vibrations are prone to jeopardize the point accuracy of the embarked sensors, they must be mitigated by using either passive or active control techniques (Sales *et al*., 2013).

(a)

(b)

Figure 1 – Illustration of dynamic vibration absorbers used helicopter: (a) applied to the main rotor (Domke, 2011); (b) positioned below the pilot seat (Krysinksi and Malburet, 2007).

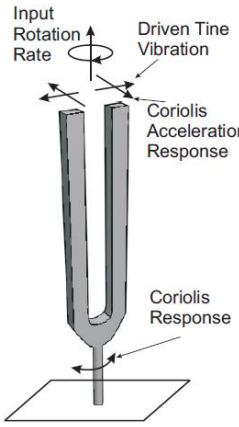

(a)

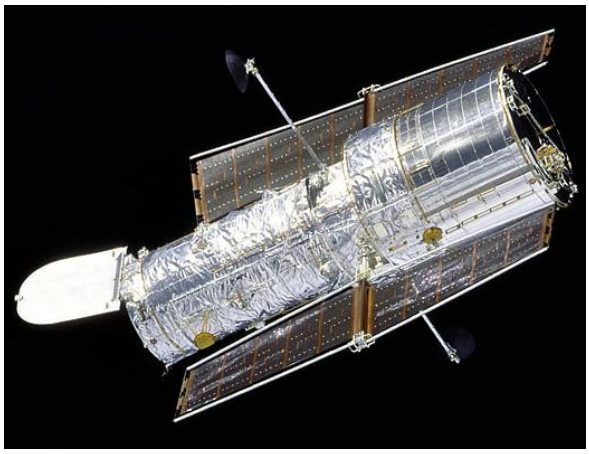

(b)

Figure 2 – Illustrations of continuous embarked vibrating systems:
(a) tuning fork-type Coriolis gyroscope (Shkel, 2006); (b): flexible panels of artificial satellites (NASA, 1997).

In this paper, the dynamics of embarked dynamic systems is addressed, both theoretically and numerically. First, the expressions of the four components of inertia forces are obtained for a particle in motion with respect to non-inertial reference frame undergoing general three-dimensional motion. Those equations are then particularized for a single-mass three degree of freedom oscillator embarked in a vehicle undergoing general motion in space and simplified further for the case of a single-mass two degree-of-freedom oscillator embarked in a vehicle performing rotation about a fixed axis. For this later case, numerical simulations are performed to demonstrate the influence of the vehicle motion on the dynamic behavior of the vibrating systems, in terms of vibration response and stability.

EQUATIONS OF MOTION FOR A PARTICLE IN A NON-INERTIAL REFERENCE FRAME

An *inertial reference frame*, or *Galilean reference frames*, is defined as one for which Newton's First Law holds, i.e., a particle free of forces is observed at rest or moving with constant velocity following a rectilinear trajectory with respect to this reference frame. In association with this definition, a force is understood as the manifestation of the interaction between the particle and the surrounding bodies. On the other hand, *non-inertial* are those to which the previous definition does not apply (Johns, 2011).

It has been shown, from Astrophysics experiments, that a reference frame fixed to the distant stars observed in the sky is an inertial reference frame (Fey *et al*., 2004). In addition, any other reference frame moving in translation at constant speed with respect to this frame is also an inertial reference frame. Obviously, as the Earth undergoes a complex motion with respect to the distant stars, composed of translation and rotations, any reference frame fixed to the Earth is not an inertial reference frame, which means that Newton's First Law is not strictly applicable to motions observed from reference frames attached to the Earth.

The idea followed herein is that, for the formulation of the equations of motion for a particle with respect to non-inertial reference frames, Newton's Second Law and derived principles can be used as long as the concept of force is extended to include two types of those, namely:

- *Interaction forces*: those originally conceptualized in Newtonian mechanics, which are due to the interactions of the particle with other bodies. They can be either volume forces (e.g. gravitational, electrostatic, electromagnetic forces) or contact forces (e.g. friction, pressure, aerodynamic forces). The interaction forces do not depend on the state of motion of the reference frame and, therefore, are invariant on the use of inertial or non-inertial reference frames.
- *Inertia forces*: those that cannot be attributed to the interaction of the particle with other bodies; their effects are

perceived only by observers based on non-inertial reference frames (Johns, 2011).

Next, it will be demonstrated that, for the most general motion a non-inertial reference frame can possibly perform, at most, four inertia forces.

Figure 3 shows a particle ***P*** of mass *m*, observed from two different reference frames, namely: the inertial frame *OXYZ*, to which the observer ***I*** is associated, and the non-inertial frame *Axyz*, whose origin follows an arbitrary trajectory in space, while it rotates with instantaneous angular velocity $\vec{\Omega}$ and angular acceleration $\dot{\vec{\Omega}}$. The observer **N** is associated to the system *Axyz*.

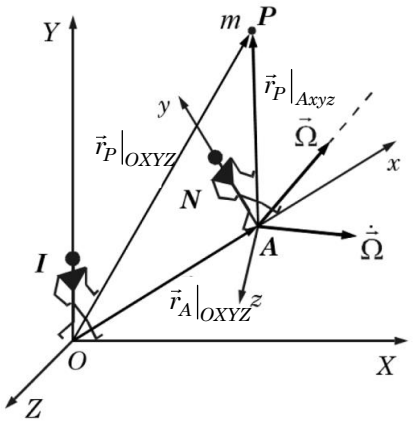

Figure 3 – Illustration of a particle moving with respect to an inertial and a non-inertial reference frame.

Based on the kinematics of relative motion with respect to moving tridimensional reference frames, the accelerations of particle ***P*** with respect to the two reference frames considered are related to each other according to (Johns, 2011):

$$\vec{a}_P\big|_{OXYZ} = \vec{a}_A\big|_{OXYZ} + \vec{a}_P\big|_{Axyz} + \dot{\vec{\Omega}}\times\vec{r}_P\big|_{Axyz} + \vec{\Omega}\times\left(\vec{\Omega}\times\vec{r}_P\big|_{Axyz}\right) + 2\vec{\Omega}\times\vec{v}_P\big|_{Axzy} \tag{1}$$

where $\vec{a}_P\big|_{OXYZ}$ and $\vec{a}_A\big|_{OXYZ}$ are, respectively, the accelerations of the particle ***P*** and point ***A***, both with respect to the inertial reference frame, $\vec{a}_P\big|_{Axyz}$ is the acceleration of particle ***P*** with respect to the non-inertial reference frame. Moreover, vectors $\dot{\vec{\Omega}}\times\vec{r}_P\big|_{Axyz}$ and $\vec{\Omega}\times\left(\vec{\Omega}\times\vec{r}_P\big|_{Axyz}\right)$ can be interpreted as the components of the acceleration, with respect to the inertial frame, of a point instantaneously coincident with point ***P***, and which is fixed with respect to the non-inertial reference frame, and $2\vec{\Omega}\times\vec{v}_P\big|_{Axzy}$ is known as Coriolis acceleration.

For the inertial reference system, Newton's Second Law is expressed as:

$$\sum\vec{F}_{int} = m\vec{a}_A\big|_{OXYZ}, \tag{2}$$

where $\sum\vec{F}_{int}$ designates the vector sum of the interaction forces applied to the particle.

On the other hand, for the non-inertial reference frame, one writes:

$$\sum\vec{F}_{int} + \sum\vec{F}_{ine} = m\vec{a}_P\big|_{Axyz}, \tag{3}$$

where $\sum\vec{F}_{ine}$ denotes the vector sum of the inertia forces.

Subtracting Eq. (2) and Eq. (3), and making use of Eq. (1), one finds the sum of the inertia forces $\sum\vec{F}_{ine}$ comprises four vectors, as follows:

$$\sum\vec{F}_{ine} = -m\vec{a}_A\big|_{OXYZ} - m\dot{\vec{\Omega}}\times\vec{r}_P\big|_{Axyz} - m\vec{\Omega}\times\left(\vec{\Omega}\times\vec{r}_P\big|_{Axyz}\right) - m\,2\vec{\Omega}\times\vec{v}_P\big|_{Axzy} \tag{4}$$

Here the following notation and terminology proposed by the Hungarian physicist and mathematician Cornelius Lanczos (1893-1974) will be used for the inertia forces:

$$\sum\vec{F}_{ine} = \vec{\varepsilon} + \vec{\varepsilon}' + \vec{C} + \vec{C}'$$

where:

$\vec{\varepsilon} = -m\,\vec{a}_A\big|_{OXYZ}$ is the Einstein's force, (5.a)

$\vec{\varepsilon}\,' = -m\dot{\vec{\Omega}}\times\vec{r}_P\big|_{Axyz}$ is the Euler's force, (5.b)

$\vec{C} = -m\vec{\Omega}\times\left(\vec{\Omega}\times\vec{r}_P\big|_{Axyz}\right)$ is the centrifugal force, (5.c)

$\vec{C}\,' = -m\,2\vec{\Omega}\times\vec{v}_P\big|_{Axyz}$ is the Coriolis' force. (5.d)

From Eqs. (5.a) to (5.d) it can be easily noticed that the inertia forces are determined by the motion of the non-inertial reference frame with respect to the inertial reference frame, i.e. on the acceleration of its origin $\vec{a}_A\big|_{OXYZ}$, on its angular velocity $\vec{\Omega}$ and angular acceleration $\dot{\vec{\Omega}}$, and also on the position and velocity of the particle with respect to the non-inertial frame, $\vec{r}_P\big|_{Axyz}$ and $\vec{v}_P\big|_{Axzy}$.

At this point, the following comments must be done: *i*) since the non-inertial system *Axyz* was assumed to perform the most general form of motion, it can be concluded that no other inertia force besides those defined in Eqs. (5) exists; *ii*) equation (3) can be interpreted as the form of Newton's Second Law to be used to obtain the equations of motion of a particle observed from non-inertial reference frames. It can be used to derive the mathematical models for the motion of embarked vibrating systems with respect a reference frame fixed to the vehicle. Those systems can be either discrete or continuous; in the latter case, as the inertia forces are directly dependent on the particle mass, they can be considered as volume forces in the derivation of the local differential equations of motion.

GENERAL EQUATIONS OF MOTION FOR A 3-DOF DISCRETE VIBRATING SYSTEM ACCOUNTING FOR INERTIA FORCES

Among a variety of situations that can be found in practical problems, this paper deals with the one illustrated in Fig. 4, in which a single-mass linear oscillator is embarked in a vehicle that undergoes general motion in space. Two references frames are considered: *OXYZ*, which is assumed to be inertial, and *Axyz*, which is fixed to vehicle, its origin being coincident with the equilibrium position of the oscillator mass. In addition, $\vec{\Omega}$ and $\dot{\vec{\Omega}}$ denote, respectively, the angular velocity and angular acceleration of the vehicle with respect to an inertial reference frame, and the suspension of the mass *m* is composed of three linear spring-viscous damper sets, denoted by $(k_x,c_x),(k_y,c_y),(k_z,c_z)$. It must be emphasized that the origin of reference frame *Axyz* is assumed to be coincident with the equilibrium position of the mass. Moreover, the orientation of the reference frame can be chosen arbitrarily with respect to the vehicle,

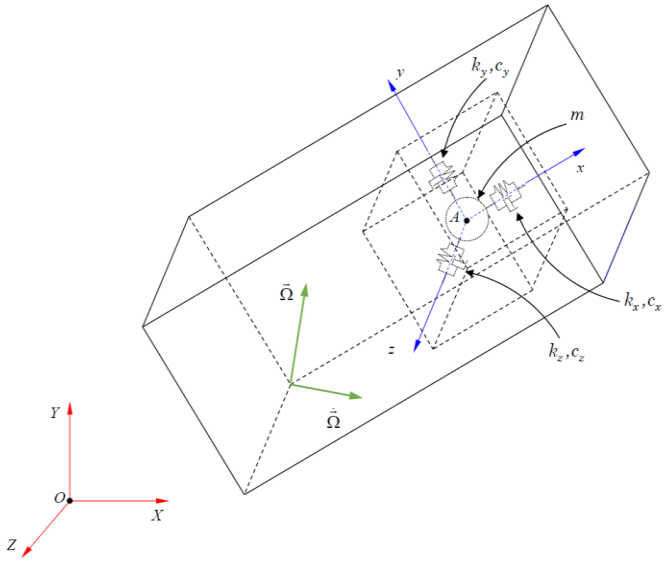

Figure 4 – Illustration of a particle moving with respect to an inertial and a non-inertial reference frame.

The interest here is to obtain the equations of motion of the mass with respect the reference frame attached to the vehicle, *Axyz*, in terms of the displacement, velocity and acceleration components in the directions those axes. Hence, from Eq. (3), one obtains the equations of motion in the form:

$$
\begin{aligned}
m\left(\ddot{x}\,\vec{i}+\ddot{y}\,\vec{j}+\ddot{z}\,\vec{k}\right) = {} & F_x\,\vec{i}+F_y\,\vec{j}+F_z\,\vec{k}-k_x x\,\vec{i}-k_y y\,\vec{j}-k_z z\,\vec{k}-c_x\dot{x}\,\vec{i}-c_y\dot{y}\,\vec{j}-c_z\dot{z}\,\vec{k}- \\
& m\left(\ddot{X}_A\,\vec{i}+\ddot{Y}_A\,\vec{j}+\ddot{Z}_A\,\vec{k}\right)-m\left(\dot{\Omega}_x\,\vec{i}+\dot{\Omega}_y\,\vec{i}+\dot{\Omega}_z\,\vec{i}\right)\times\left(x\,\vec{i}+y\,\vec{j}+z\,\vec{k}\right)- \\
& m\left(\Omega_x\,\vec{i}+\Omega_y\,\vec{i}+\Omega_z\,\vec{i}\right)\times\left[\left(\Omega_x\,\vec{i}+\Omega_y\,\vec{i}+\Omega_z\,\vec{i}\right)\times\left(x\,\vec{i}+y\,\vec{j}+z\,\vec{k}\right)\right]- \\
& 2\left(\Omega_x\,\vec{i}+\Omega_y\,\vec{i}+\Omega_z\,\vec{i}\right)\times\left(\dot{x}\,\vec{i}+\dot{y}\,\vec{j}+\dot{z}\,\vec{k}\right),
\end{aligned}
\tag{6}
$$

where $F_x(t), F_y(t), F_z(t)$ are the components of interaction excitation forces applied to the mass, $x(t), y(t), z(t)$ and $\dot{x}(t), \dot{y}(t), \dot{z}(t)$ are, respectively, the components of the position and velocity of the mass with respect to the reference frame *Axyz*, $\ddot{X}_A(t), \ddot{Y}_A(t), \ddot{Z}_A(t)$ are the components of the acceleration of the origin of the reference frame *Axyz* with respect to the inertial frame, $\Omega_x(t), \Omega_y(t), \Omega_z(t)$ and $\dot{\Omega}_x(t), \dot{\Omega}_y(t), \dot{\Omega}_z(t)$ are, respectively, the components of the angular velocity and angular acceleration of the vehicle with respect to the inertial reference frame.

From Eq. (6), it can be seen that the motion of the mass with respect to the reference frame attached to the vehicle is dictated not only by the interaction excitation forces applied to it, but also by the inertia forces, which, on their turn, depend on the motion of the vehicle. Therefore, this dynamics tend to be complex and interesting behavior can be observed.

To put these phenomena in evidence, in the next section, the three-dimensional situation depicted in Fig. 5 will be particularized to a two-dimensional case. Based on the theory developed above, the equations of motion are derived for particular cases of linear vibrating discrete systems embarked in a vehicle undergoing rotation about a fixed axis.

EQUATIONS OF MOTION FOR A 2-DOF DISCRETE VIBRATING SYSTEM, EMBARKED IN A ROTATING VEHICLE, ACCOUNTING FOR INERTIA FORCES

Figure 5 depicts a 2 DOF vibrating system composed by a point mass *m* connected by linear springs (k_1, k_2) and viscous dampers (c_1, c_2) to a vehicle which rotates in a horizontal plane about the axis orthogonal to it, passing through point *O*, with instantaneous angular velocity $\vec{\Omega}(t)=\dot{\theta}(t)\vec{k}$ and angular acceleration $\dot{\vec{\Omega}}(t)=\ddot{\theta}(t)\vec{k}$.

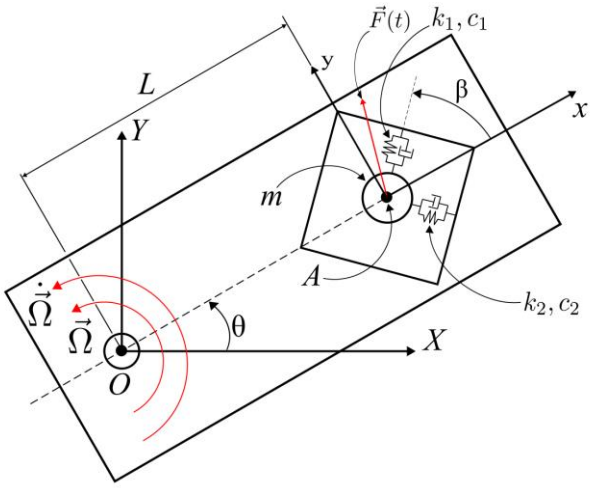

Figure 5 – Illustration of a 2 DOF vibrating system embarked in a rotating vehicle.

In Fig. 5, the reference frame *OXYZ* is assumed to be fixed (inertial), while the reference frame *Axyz* is attached to the vehicle, having its origin coincident with the equilibrium position of the mass, denoted by *A*. The angle β is introduced to account for the orientation of the suspension with respect to the axes of the reference frame *Axyz*.

For this case, the equations of motion, obtained from Eq. (6), are given as:

$$
\ddot{\boldsymbol{u}}(t)+\tilde{\boldsymbol{C}}\dot{\boldsymbol{u}}(t)+\tilde{\boldsymbol{K}}\boldsymbol{u}(t)=\tilde{\boldsymbol{F}}(t) \tag{7}
$$

where:

$$
\boldsymbol{u}(t)=\left[x(t)\quad y(t)\right]^T \tag{8.a}
$$

$$\tilde{\boldsymbol{C}} = \begin{bmatrix} 2\zeta_1\omega_1 \cos^2\beta + 2\zeta_2\omega_2 \sin^2\beta & 2\left(\zeta_1\omega_1 - \zeta_2\omega_2\right)\sin\beta\cos\beta - 2\Omega \\ 2\left(\zeta_1\omega_1 - 2\zeta_2\omega_2\right)\sin\beta\cos\beta + 2\Omega & 2\zeta_1\omega_1 \sin^2\beta + 2\zeta_2\omega_2 c\cos^2\beta \end{bmatrix} \tag{8.b}$$

$$\tilde{\boldsymbol{K}} = \begin{bmatrix} \omega_1^2 \cos^2\beta + \omega_2^2 \sin^2\beta - \Omega^2 & \left(\omega_1^2 - \omega_2^2\right)\sin\beta\cos\beta - \dot{\Omega} \\ \left(\omega_1^2 - \omega_2^2\right)\sin\beta\cos\beta + \dot{\Omega} & \omega_1^2 \sin^2\beta + \omega_2^2 \cos^2\beta - \Omega^2 \end{bmatrix}, \quad \tilde{\boldsymbol{F}} = \begin{Bmatrix} F_x(t) + L\Omega^2 \\ F_y(t) - L\dot{\Omega} \end{Bmatrix} \tag{8.c}$$

$$\omega_1 = \sqrt{k_1/m}, \omega_2 = \sqrt{k_2/m}, \zeta_1 = c_1/\left(2\sqrt{k_1 m}\right), \zeta_2 = c_2/\left(2\sqrt{k_2 m}\right)$$

In Eqs. (7)-(8), it can be seen that: *i*) the system matrices depend on the values of the angular velocity and angular acceleration of the vehicle. Hence, it is expected that these parameter exert influence on the dynamic features (modal characteristics, time and frequency responses) of the vibrating system; *ii*) the equations of motion are coupled, not only due to influence of the angle β but also due to the angular velocity and angular acceleration of the vehicle that appear in the off-diagonal terms of matrices $\tilde{\boldsymbol{C}}$ and $\tilde{\boldsymbol{K}}$; *iii*) in the cases where either Ω or $\dot{\Omega}$ vary with time, the equations of motion involve time-depend coefficients; *iv*) the rotation of the vehicle induces the appearance of excitation forces, which are added to the external excitation forces in the right-hand-side of Eq. (7).

NUMERICAL SIMULATIONS

In order to characterize the dynamics of the embarked vibrating systems undergoing plane motion, and demonstrate the influence of the vehicle motion on this dynamics, in this section, the results of numerical simulations based on the integration of Eqs. (8)-(9) are presented for particular characteristics of the vehicle motion. The following values of the vibrating system parameters are considered: $\omega_1 = 100$ rad/s, $\omega_2 = 200$ rad/s, $\zeta_1 = 0.01$, $\zeta_2 = 0.02$, L=0.1m.

First case: vehicle rotating at constant angular velocity

In the first case one considers the vehicle rotating at constant speed and investigates the influence of the value of the angular velocity on the dynamic response of the vibrating system in terms of its natural frequencies and free response to an arbitrarily chosen set of initial conditions, for a particular orientation angle $\beta = 30^o$.

Figure 6 shows the variations of the real and imaginary parts of the eigenvalues associated to Eq. (7), for the undamped vibrating system ($\zeta_1 = \zeta_2 = 0$), whilst Figure 7 shows similar results for the damped system ($\zeta_1 = 0.01$, $\zeta_2 = 0.02$). It can be seen that, for the undamped system, in the range $\left[\omega_1 \le \Omega \le \omega_2\right]$ the motion becomes unstable (as indicated by the occurrence of eigenvalues with positive real parts), while it is stable for all other values of the rotation speed. On the other hand, for the damped system, instability occurs in the interval $\left[\Omega \ge \omega_1\right]$, which shows that the addition of viscous damping has a detrimental effect on the system stability.

These results corroborate the linear stability conditions obtained from the Routh-Hurwitz criterion (Ogata, 2010), which is not presented here.

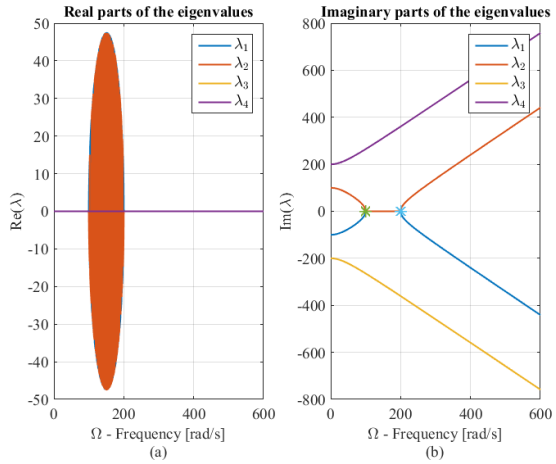

Figure 6 – Real and imaginary parts of the eigenvalues associated to Eq. (7) as functions of Ω for $\omega_1 = 100$ rad/s, $\omega_2 = 200$ rad/s, $\zeta_1 = 0$, $\zeta_2 = 0$, $L = 0.1$m, $\beta = 30^o$.

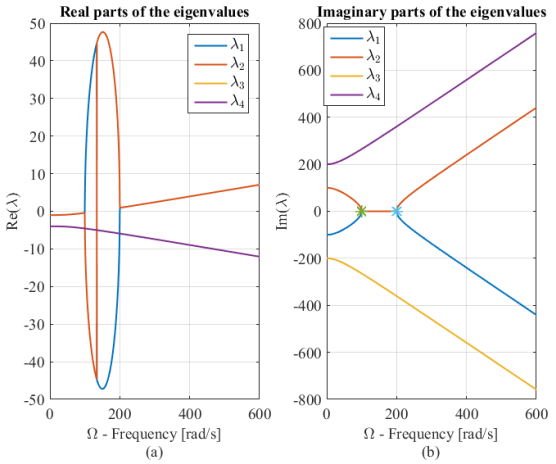

Figure 7 – Real and imaginary parts of the eigenvalues associated to Eq. (7) as functions of Ω for $\omega_1 = 100$ rad/s, $\omega_2 = 200$ rad/s, $\zeta_1 = 0.01$, $\zeta_2 = 0.02$, $L = 0.1$m, $\beta = 30^o$.

Figures 8 to 11 illustrate the free response time histories and corresponding orbits of the undamped vibrating system for null initial conditions $\left(x(0)=y(0)=0.0\,\mathrm{m}\right)$, for some values of the rotation speed selected in the stability zone. Similar results are presented in Figs. 12 and 13 for the viscously damped system.

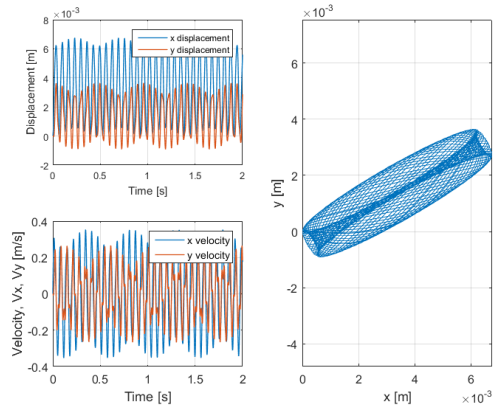

Figure 8 – Response time histories and motion orbit for $\omega_1 = 100$ rad/s, $\omega_2 = 200$ rad/s, $\zeta_1 = 0$, $\zeta_2 = 0$, $L = 0.1\,\mathrm{m}$, $\beta = 30^{\circ}$ and $\Omega = 20\,\mathrm{rad/s}$.

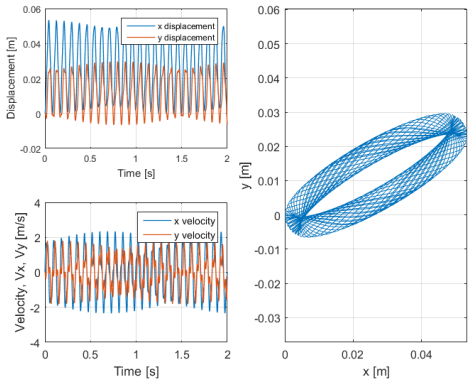

Figure 9 – Response time histories and motion orbit for $\omega_1 = 100$ rad/s, $\omega_2 = 200$ rad/s, $\zeta_1 = 0$, $\zeta_2 = 0$, $L = 0.1\,\mathrm{m}$, $\beta = 30^{\circ}$ and $\Omega = 50\,\mathrm{rad/s}$.

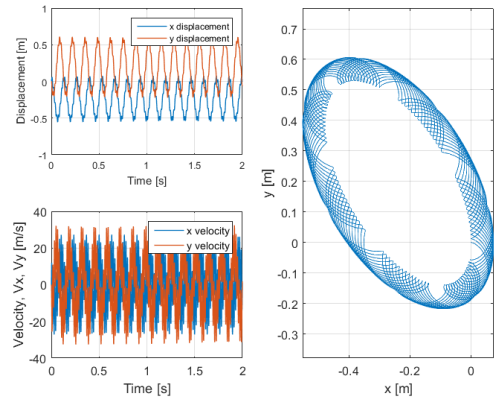

Figure 10 – Response time histories and motion orbit for $\omega_1 = 100$ rad/s, $\omega_2 = 200$ rad/s, $\zeta_1 = 0$, $\zeta_2 = 0$, $L = 0.1\,\mathrm{m}$, $\beta = 30^{\circ}$ and $\Omega = 220\,\mathrm{rad/s}$.

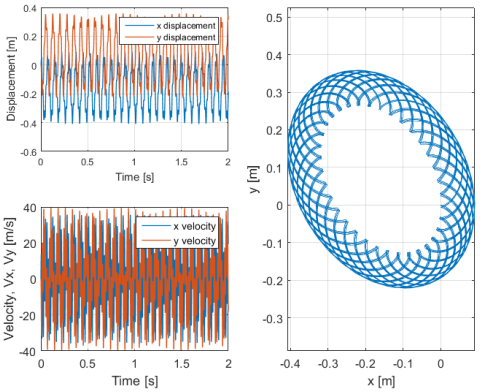

Figure 11 – Response time histories and motion orbit for $\omega_1 = 100$ rad/s, $\omega_2 = 200$ rad/s, $\zeta_1 = 0$, $\zeta_2 = 0$, $L = 0.1\,\mathrm{m}$, $\beta = 30^{\circ}$ and $\Omega = 250\,\mathrm{rad/s}$.

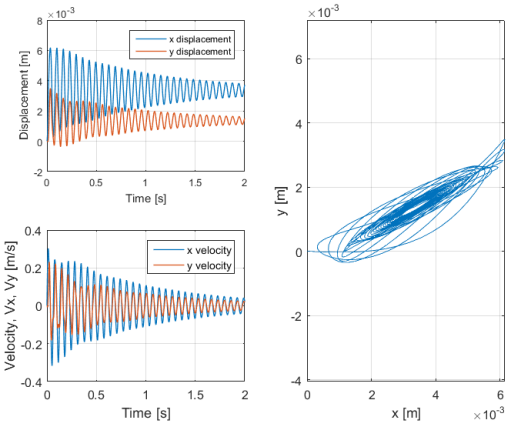

Figure 12 – Response time histories and motion orbit for $\omega_1 = 100$ rad/s, $\omega_2 = 200$ rad/s, $\zeta_1 = 0.01$, $\zeta_2 = 0.02$, $L = 0.1\,\mathrm{m}$, $\beta = 30^{\circ}$ and $\Omega = 20\,\mathrm{rad/s}$

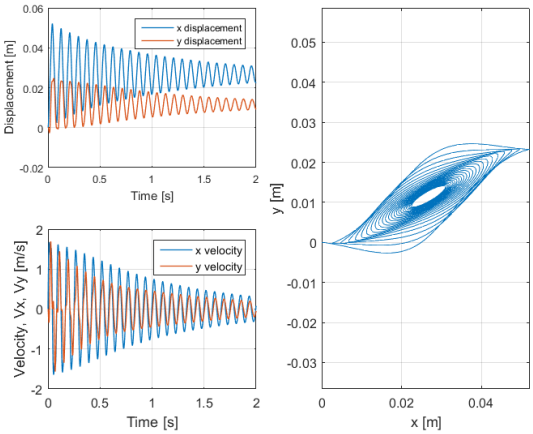

Figure 13 – Response time histories and motion orbit for $\omega_1 = 100$ rad/s, $\omega_2 = 200$ rad/s, $\zeta_1 = 0.01$, $\zeta_2 = 0.02$, $L = 0.1\,\mathrm{m}$, $\beta = 30^{\circ}$ and $\Omega = 50\,\mathrm{rad/s}$.

In Figs. 8 to 13, it can be seen that the features of the free response of the vibrating system, in terms of amplitude, period of oscillation and coupling between *x* and *y* components (which defines the motion orbit) are very diverse, depending on the value of the angular velocity of the vehicle. In particular, the vibration amplitudes tend to be excessively large when the angular velocity of the vehicle is large (Figs. 10 and 11), which can, in practice, induce nonlinear behavior of the springs.

Next, the influence of the orientation angle β on the vibration response of the oscillator is evaluated. Figures 14 to 17 depict the responses of the damped system, for four different values of this angles, for null initial conditions $\left(x(0)=y(0)=0.0\,\mathrm{m}\right)$.

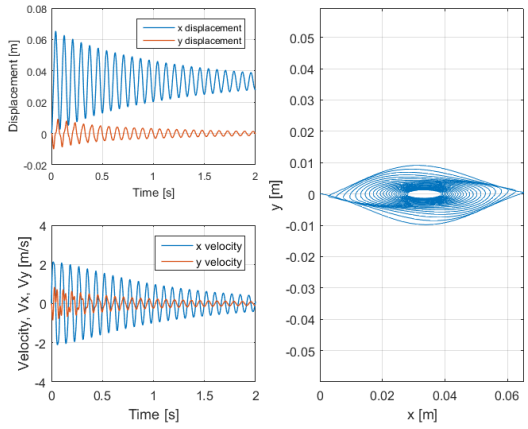

Figure 14 – Response time histories and motion orbit for $\omega_1=100\ \mathrm{rad/s}$, $\omega_2=200\ \mathrm{rad/s}$, $\zeta_1=0.01$, $\zeta_2=0.02$, $L=0.1\,\mathrm{m}$, $\beta=0^{\mathrm{o}}$ and $\Omega=50\ \mathrm{rad/s}$.

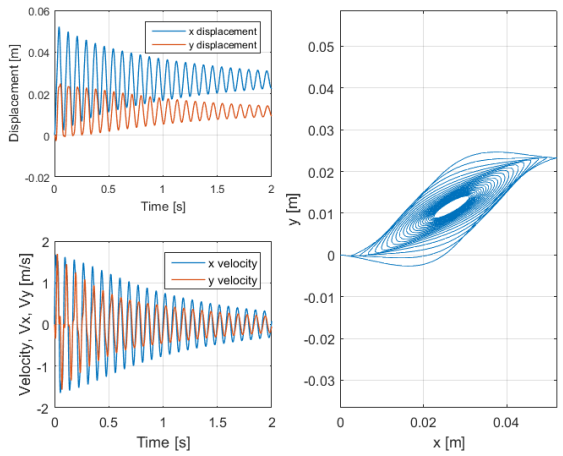

Figure 15 – Response time histories and motion orbit for $\omega_1=100\ \mathrm{rad/s}$, $\omega_2=200\ \mathrm{rad/s}$, $\zeta_1=0.01$, $\zeta_2=0.02$, $L=0.1\,\mathrm{m}$, $\beta=30^{\mathrm{o}}$ and $\Omega=50\ \mathrm{rad/s}$.

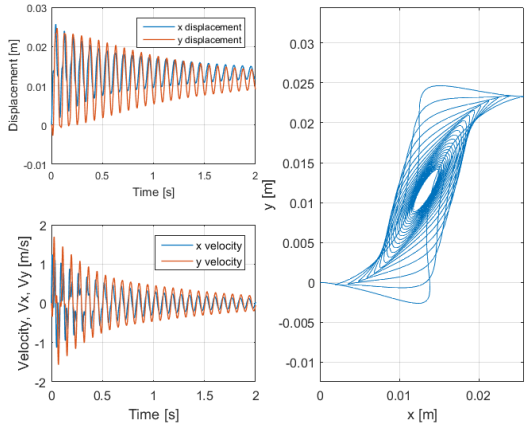

Figure 16 – Response time histories and motion orbit for $\omega_1=100\ \mathrm{rad/s}$, $\omega_2=200\ \mathrm{rad/s}$, $\zeta_1=0.01$, $\zeta_2=0.02$, $L=0.1\,\mathrm{m}$, $\beta=60^{\mathrm{o}}$ and $\Omega=50\ \mathrm{rad/s}$.

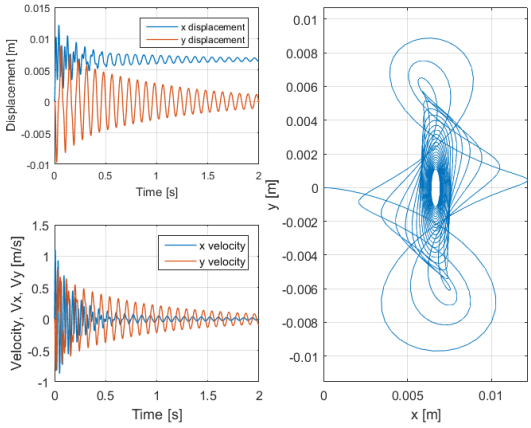

Figure 17 – Response time histories and motion orbit for $\omega_1=100\ \mathrm{rad/s}$, $\omega_2=200\ \mathrm{rad/s}$, $\zeta_1=0.01$, $\zeta_2=0.02$, $L=0.1\,\mathrm{m}$, $\beta=90^{\mathrm{o}}$ and $\Omega=50\ \mathrm{rad/s}$.

In Figs. 14 to 17, it can be seen that the influence of the orientation of the suspension with respect to the vehicle cannot be represented by a simple geometric coordinate rotation of the orbits by the corresponding orientation angle.

Second case: vehicle rotating with linearly varying rotation speed

From Eqs. (7) and (8) one can see that when the angular velocity of the vehicle varies with time, the angular acceleration $\dot{\Omega}$, associated to the Euler's force, appears in the off-diagonal terms of matrix $\tilde{\boldsymbol{K}}$, thus promoting additional coupling between coordinates *x* and *y*. Furthermore, the non-zero angular acceleration induces addition forcing terms in the right-hand-side of Eq. (7). This case is examined next, assuming that the angular acceleration of the vehicle is constant, so that its angular velocity varies linearly with time according to $\Omega(t)=\Omega_0+\dot{\Omega}t\left[\mathrm{s;rad/s}\right]$.

Figure 18 illustrates the free response time histories and corresponding orbit of the undamped vibrating system, for initial conditions $\left(x(0)=y(0)=0.005\ \mathrm{m}\right)$, $\Omega_0=0.0\,\mathrm{rad/s}$, $\dot{\Omega}=10\,\mathrm{rad/s^2}$ (run-up) the time interval $\left[0;5\mathrm{s}\right]$, while Fig. 19 depicts the responses for $\Omega_0=50\,\mathrm{rad/s}$, $\dot{\Omega}=-10\,\mathrm{rad/s^2}$ (run-down), with the same initial conditions and

observation interval.

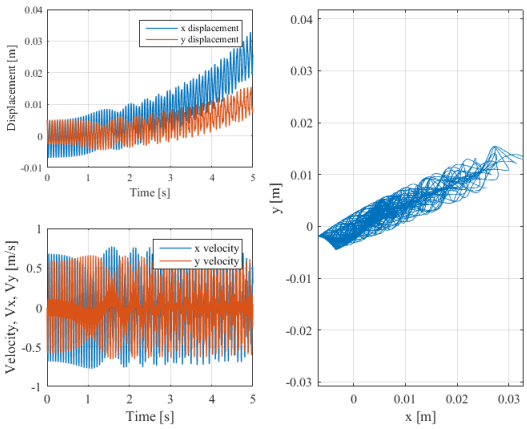

Figure 18 – Response time histories and motion orbit for $\omega_1 = 100\ \text{rad/s}$, $\omega_2 = 200\ \text{rad/s}$, $\zeta_1 = 0.0$, $\zeta_2 = 0.0$, $L = 0.1\,\text{m}$, $\beta = 30^\text{o}$, $\Omega_0 = 0.0\,\text{rad/s}$, $\dot{\Omega} = 10\,\text{rad/s}^2$

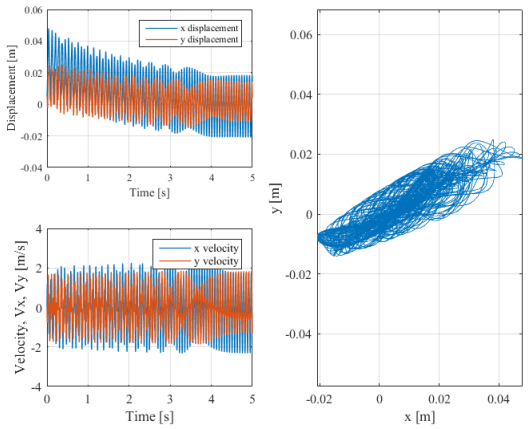

Figure 19 – Response time histories and motion orbit for $\omega_1 = 100\ \text{rad/s}$, $\omega_2 = 200\ \text{rad/s}$, $\zeta_1 = 0.0$, $\zeta_2 = 0.0$, $L = 0.1\,\text{m}$, $\beta = 30^\text{o}$, $\Omega_0 = 50.0\,\text{rad/s}$, $\dot{\Omega} = -10\,\text{rad/s}^2$.

The results shown in Figs. 18 and 19 show that the amplitudes of vibration tend to increase monotonically with the increase of the angular velocity of the vehicle in the run-up case, and decrease monotonically for the run-down case.

CONCLUSIONS

From the theoretical standpoint, a general procedure for the derivation of the equations of motion of vibrating systems with respect to non-inertial reference frames, based on the concept of inertial forces, was suggested. This procedure was applied to describe the motion of a single mass, three-degree-of-freedom damped oscillator embarked in a vehicle undergoing general three-dimensional motion, with respect to a non-inertial reference frame attached to the vehicle. Those equations were then particularized for the case in which a single mass, two-degree-of-freedom oscillator is embarked in a vehicle rotating about a fixed axis.

It was made evident that the rotation parameters of the vehicle (Ω or $\dot{\Omega}$), as well as geometrical parameters that define the position and orientation of the oscillator in the vehicle (L and β, respectively) intervene in the equations of motion and, as a result, are expect to exert influence on the characteristics of the dynamic response.

A number of numerical simulations performed by integrating the equations of motion were carried-out to illustrate the influence of those rotation and geometric parameters on the motion of the oscillator. Although somewhat limited, those simulations enabled to demonstrate the existence of intervals of the rotation speed Ω for which the motion becomes unstable. It was also shown that, in the stability zones, the features of the dynamic response (amplitude and coupling between x and y motions) depend strongly on the rotation speed and orientation of the suspension of the oscillator with respect to the vehicle. That dependency must be duly accounted for in the phases of analysis and design of embarked vibrating systems.

Besides the theoretical interest in the problem addressed herein, the authors believe that theory and results presented in this paper can be useful in the analysis and design of vibrating devices found in many practical applications.

ACKNOWLEDGMENTS

D.A. Rade is grateful to CNPq (projects numbers 310633/2013-3 and 402238/2013-3) and FAPESP (project number 2015/20363-6) for the financial support to his research work. E. Spuldaro express his gratitude to FAPESP for his M.Sc. scholarship (project number 2016/16480-0). L.F. Damy is grateful to the Brazilian Army for supporting his M.Sc. research, providing data and resources.

REFERENCES

Apostolyuk, V., 2016, Coriolis Vibratory Gyroscopes: theory and design, Springer, Switzerland, 122 p.

Domke, B., 2011, Aviation Images, available in: <http://www.b-domke.de/AviationImages.html>, access in August 1, 2016.

Fey, A. L., 2004, The Second Extension of the International Celestial Reference Frame: ICRF-EXT. 1, The Astronomical Journal, Vol. 127, No. 6, pp. 3587-3608.

Johns, O. D., 2011, Analytical Mechanics for Relativity and Quantum Mechanics: Part I, Oxford University Press, Oxford, England, UK, 634 p.

Krysinksi, T. and Malburet, F., 2007, Mechanical Vibrations: active and passive control, ISTE, Newport Beach, USA, 389 p.

NASA, 1997, The Hubble Space Telescope, available in: <http://hubblesite.org/gallery/spacecraft/03/>, access in August 1, 2016.

Ogata, K., 2010, Modern Control Engineering, Prentice Hall, 5th. ed, Upper Saddle River, New Jersey, USA, 389 p.

Sales, T. P., 2013, Passive vibration control of flexible spacecraft using shunted piezoelectric transducers, Journal of Aerospace Science and Technology, Vol. 29, No. 1, pp. 403-412.

Shkel, A. M., 2006, Type I and Type II Micromachined Vibratory Gyroscope, Proceedings of 2006 IEEE/ION Position, Location and Navigation Symposium, San Diego, CA, USA, pp. 586-593.

RESPONSIBILITY NOTICE

The authors are the only responsible for the material included in this paper.